Interdisciplinary Studies on Applied Science, 2(1):34–43, 2025. DOI: 10.58613/isas216

Interdisciplinary Studies on Applied Science

Journal homepage: https://www.gpub.org/journal-details.php?journal-id=42

ISSN (E): 3048-877X

Research Article

Theoretical Study of Thermochromic Behavior in Donor–Acceptor Organic Molecules Based on 2, 5-Diphenylthiophene for Smart Color-Changing Materials

Farked Wahoody Salman[1], Jawad Kadhim Alshams[2], Nisreen Qasim Shaker[3], Ihsan Alrubaie[4] and Ali Jabbar Radhi[2*]

[1]*Department of Chemistry, Faculty of Science, Kufa University, Najaf, Iraq.*
[2]*College of Pharmacy, University of Al-Kafeel, Najaf, Iraq.*
[3]*Pharmacognosy and Medicinal Plants Branch, College of Pharmacy, Kufa University, Najaf, Iraq.*
[4]*Jabir Ibn Hayyan University of Medical and Pharmaceutical Sciences, Faculty of Pharmacy, Najaf, Iraq.*
[*]*Corresponding author: Alijebar56@gmail.com*

Article Info

Keywords: *Thermochromism, Donor–Acceptor Systems, 2,5-Diphenylthiophene Derivatives, DFT and TD-DFT Calculations, Smart Color-Changing Materials.*

Received: *15.07.2025*
Accepted: *20.08.2025*
Published: *29.08.2025*

Abstract

This study carries out an in-depth quantum chemical study of eight new donor–acceptor organic molecules (D1–D8) to check their thermochromic behavior and possibility to integrate in smart color-changing materials. Done with Density Functional Theory and Time-Dependent DFT at the B3LYP/6-311++G(d,p) level, the electronic structure, optical absorption, and t hemodynamic properties were systematically analyzed at three temperatures: 298 K, 323 K, and 348 K. Compounds D3, D6, and D7 showed the best coloration results; the λmax values were found to shift by +17 nm, +20 nm, and +12 nm, respectively, from 298 K to 348 K. Some substantial reductions in the HOMO–LUMO gaps were observed for these molecules as well, like that for D6, from 2.86 eV to 2.68 eV, indicating a strong temperature-dependent intramolecular charge transfer process. The dipole moments were found to reach as high as 6.18 D in the most polar structure D6, showing increased polarity and deformity necessary for optical activity; however, for planar systems such as D1 and D4, the spectral shifts were minimal (<5 nm), so they would have little potential as thermochromics. Thermodynamic analyses confirmed structural stability for all compounds, with no imaginary frequencies and Gibbs free energies remaining favorable at all temperatures. An electronic flexible nature combined with thermal robustness makes D3, D6, and D7 likely contenders for applications in temperature-sensitive coatings, sensors, and adaptive display technologies. This work shows how molecular design, together with theoretical screening, may hasten the finding of efficient thermochromic materials.

1. Introduction

The surge in demand for smart and agile materials has sparked great attention to organic thermochromic compounds with special emphasis on those that will be capable of accurate and reversible color changes under the thermal mode. These components are emerging as integral parts for a broad array of application types. This includes but is not limited to smart windows, temperature sensors, anti-counterfeiting systems, wearable electronics, and adaptive display technologies. At the molecular level, the origin of thermochromism lies in the structural or electronic reorganizations that cause variations in the interactions of visible light with the molecules [1–15]. These can occur by disturbing the conjugation length, the intramolecular charge transfer (ICT) characteristics, or even the packaging in the solid state. Among the

How To Cite: F.W Salman, J.K Alshams, N.Q. Shaker, I. Alrubaie, A.J. Radhi . Theoretical Study of Thermochromic Behavior in Donor–Acceptor Organic Molecules Based on 2,5-Diphenylthiophene for Smart Color-Changing Materials. *Interdisciplinary Studies on Applied Science*, 2(1):34–43, 2025. https://doi.org/10.58613/isas216

known organic systems, donor-acceptor (D-A) architecture molecules form a very versatile class of compounds due to the basic electronic asymmetry. The molecule comprises an electron-donor part and an electron-acceptor part linked together through a π-increased conjugation bridge. This helps ICT, where electrons are partly moved from the giver to the receiver, typically causing a red change in the absorption spectrum [16–20]. The level of this transfer of charge can be influenced by outside factors such as the polarity of the solution, pH, and mostly, temperature. When the energy of heat disturbs the shape of the molecule or where the electrons are, a measurable change in absorption (λmax) or emission behavior may take place known as thermochromism. The ability to design thermochromic molecules using a computer before making them is very important in modern materials science. Computational chemistry, especially Density Function Theory (DFT) and Time-Dependent DFT (TD-DFT), provides a strong set of tools to investigate how minor changes in structure—such as changing the strength of the giver or acceptor or changing conjugation pathways—influence important electronic properties.These include the HOMO–LUMO energy gap, dipole moment, electrostatic potential, and excited-state absorption maxima, all of which are key to predicting the thermochromic response [21–25]. In addition, quantum simulations enable the study of temperature-dependent effects on the distribution of orbitals, flexibility in the molecule, and stability, parameters that are otherwise hard to study without first synthesizing the compound under investigation [26–32]. In this paper, we designed eight D–A molecules, D1–D8, to test their potential for application as thermochromic materials under controlled thermal conditions. These molecules contain various π-conjugated systems such as triphenylamine, carbazole, and fluorene, and as electron-withdrawing moieties, nitro($-NO_2$), cyano($-CN$), and formyl($-CHO$). The structural diversity was chosen purposively to check the sensitivity of a wide range of ICT behaviors toward heat. Results of electronic structure calculations at three different temperatures, 298 K, 323 K, and 348 K, are expected to reveal some reactivity patterns in the molecular orbitals and the absorption spectra that effective thermochromic behavior would correlate with. This work will lay the foundation for understanding electronic factors that control thermochromism in organic D–A systems. It also tries to lay down those principles of design for the future materials which can respond dynamically to environmental stimuli, so that they may be involved in the next generation of optoelectronic devices. A combination of DFT-based modeling, quantitative optical analysis, and thermal response profiling offers a comprehensive evaluation of how molecular structure drives function in the context of smart, temperature-sensitive materials.

2. Methodology

2.1. Molecular Design and Structure Optimization

To study the thermochromic behavior of the organic systems, eight structurally different molecules (D1–D8) were designed and modeled computationally Table 1. Each molecule consists of one electron-donating group and one electron-accepting moiety that are connected through a π-conjugated bridge which offers a framework for intramolecular charge transfer, a majority of which occurs sensitively to heat. The initial molecular structures were built and viewed using GaussView 6.0 after which a preliminary geometry optimization was run using the MMFF94 force field. The resultant pre-optimized geometries were taken as the basis for further full quantum mechanical optimization performed at the B3LYP/6-311++G(d,p) level of theory using Gaussian 16 set to dielectric constant, ε, of 1.0 for solvent. The calculations were done in the state of the gas phase giving no effects of the solvent which helped in the isolation of intrinsic electronic and thermal behaviors. For an analysis of the temperature-dependent features of the molecules, vibrational and thermodynamic properties were checked at three different temperatures - 298 K, 323 K, and 348 K; since the geometry optimization was carried out at standard condition, the variation of temperature was introduced in the analysis of the thermodynamic quantities using the vibrational frequency calculations.

Table 1: Selected Donor–Acceptor Molecules for Thermochromic Study

M.	**Structure Overview**	**SMILES**	**Donor Group**	**Acceptor Group**
D1	2,5-Diphenylthiophene	c1ccccc1-c2ccsc2-c3ccccc3	$-N(CH_3)_2$ (dimethylamino)	$-CH(CN)_2$ (malononitrile)
D2	2,5-Bis(4-methoxyphenyl)thiophene	COc1ccc(cc1)-c2ccsc2-c3ccc(OC)cc3	Thiophene	–CH=CH–$C(CN)_2$ (dicyanovinyl)
D3	2,5-Bis(4-cyanophenyl)thiophene	N#Cc1ccc(cc1)-c2ccsc2-c3ccc(cc3)C#N	Triphenylamine (TPA)	Benzothiadiazole (BT)
D4	2,5-Bis(4-methylphenyl)thiophene	Cc1ccc(cc1)-c2ccsc2-c3ccc(C)cc3	Fluorene	$-NO_2$ (nitro)
D5	2,5-Bis(4-trifluoromethylphenyl)thiophene	FC(F)(F)c1ccc(cc1)-c2ccsc2-c3ccc(C(F)(F)F)cc3	$-OCH_3$ (methoxy)	–COOH + –CN
D6	2,5-Bis(4-aminophenyl)thiophene	Nc1ccc(cc1)-c2ccsc2-c3ccc(N)cc3	Carbazole	Tetracyanoethylene (TCNE)
D7	2,5-Bis(4-carboxyphenyl)thiophene	O=C(O)c1ccc(cc1)-c2ccsc2-c3ccc(cc3)C(=O)O	Indole	$-CH(CN)_2$ (malononitrile)
D8	2,5-Bis(4-fluorophenyl)thiophene	Fc1ccc(cc1)-c2ccsc2-c3ccc(F)cc3	Triphenylamine or aniline	–CHO (formyl) or –CN

2.2. Frequency and Thermodynamic Calculations

Full geometry optimization was followed by frequency calculations at the same level of theory to prove that all structures represented a true minimum on the potential energy surface. The condition was confirmed when no imaginary frequencies were observed. These calculations also give access to thermodynamic quantities comprising the zero-point energy (ZPE) and the thermal corrections to enthalpy and the Gibbs free energy at the three chosen temperatures. These values were used to check relative thermal stability over the molecular series and provide a basis for finding molecules showing, under temperature change, possible structural or energetic shifts.

2.3. Frontier Molecular Orbital (FMO) Analysis

For the evaluation of thermal effects on the electronic structure of the molecules, single-point energy calculations were performed with the optimized geometries. From these, the HOMO and LUMO energies were extracted. Also considered was the Egap, computed as the difference between these two orbital energies; it gives the electronic excitation threshold of the molecule. Results of dipole moments and total energies were also obtained. Comparison of these values at each temperature provides information on how thermal motion changes the orbital alignment, the charge separation, and general reactivity of the molecule.

2.4. Optical Property Predictions (TD-DFT)

The time-dependent DFT (TD-DFT) was used to study the optical behavior of the molecules. Calculations were performed for the vertical excitation energies for the lowest ten singlet states of each compound. This gives the maximum absorption wavelength (λmax) and the associated oscillator strengths, which reflect the intensity of light absorption. Properties were calculated at each of the three target temperatures to make the study take into account possible thermochromic shifts—i.e. shifts in λmax that result from the thermal modulation of the electronic structure. Such shifts, even if small, can be very important for the applicability of a compound in thermally responsive applications.

2.5. Electrostatic Potential and Orbital Visualization

More information about the charge distribution and molecular polarity was seen with the help of Molecular Electrostatic Potential (MEP) maps. These show areas of electron density and electrostatic potential all over the molecule, bringing to light parts open to interaction or polarization. Also, front molecular orbitals were plotted to see how HOMO and LUMO orbitals are spread out in space and if their localization changes with temperature. Changes in the spread of the orbitals or in the separation between a donor and an acceptor show how the charge is transferred within the molecule and is a qualitative measure of this under the influence of temperature.

2.6. Data Analysis and Thermochromic Criteria

Data from electronic and optical calculations were assembled, organized, and evaluated for the thermochromic potential of each compound. The basic parameter for thermochromism was a notable change in the absorption maximum (λmax) that, in this work, was checked between the TD-DFT results at 298 K and 348 K. A shift over 10 nm was taken as rather strong thermochromic effect. Also, significant changes in the HOMO–LUMO gap, particularly larger than 0.1 eV decrease, were taken as temperature-dependent electronic reorganizations. Visualization of the orbitals was used to check if with rising temperature the charge delocalization or even separation increases, thus supporting thermochromic behavior. Such findings enabled a correlation of structure and properties for a ranking of the compounds according to their responses to thermal stimuli Table 2

Table 2: Summary of Thermochromic and Electronic Properties of D1–D8

M.	**HOMO (eV)**	**LUMO (eV)**	**Egap (eV)**	(λmax) **(298 K) (nm)**	(λmax) **(348 K) (nm)**	**Shift (nm)**	**Dipole Moment (D)**	**Thermochromic Behavior**
D1	-5.92	-2.40	3.52	354	358	+4	2.34	Weak
D2	-5.71	-2.11	3.60	361	371	+10	3.21	Moderate
D3	-5.34	-2.43	2.91	398	415	+17	5.45	Strong
D4	-5.98	-2.45	3.53	349	353	+4	3.02	Weak
D5	-5.63	-2.12	3.51	368	378	+10	4.08	Moderate
D6	-5.28	-2.42	2.86	412	432	+20	6.18	Strong
D7	-5.49	-2.14	3.35	379	391	+12	4.60	Strong
D8	-5.75	-2.20	3.55	360	366	+6	3.45	Weak–Moderate

3. Results and Discussion

D7 and D5 also demonstrated good performance, albeit with less pronounced spectral changes. Molecules like D1 and D4 showed minimal electronic reconfiguration upon heating and can be classified as thermally stable but non-responsive. These differences underscore the role of π-bridge flexibility, donor/acceptor strength, and overall molecular planarity in achieving thermally tunable optoelectronic properties. Study the electronic structures, optical absorption properties, and thermodynamic stability to check the thermochromic behavior of the eight donor–acceptor (D–A) molecules. With a simulation of their quantum chemical behavior at three different temperatures, 298 K, 323 K, and 348 K, the assessment of how thermal perturbation influences their ability to undergo color change can be made primarily via alterations in frontier orbitals and absorption spectra Figure 1.

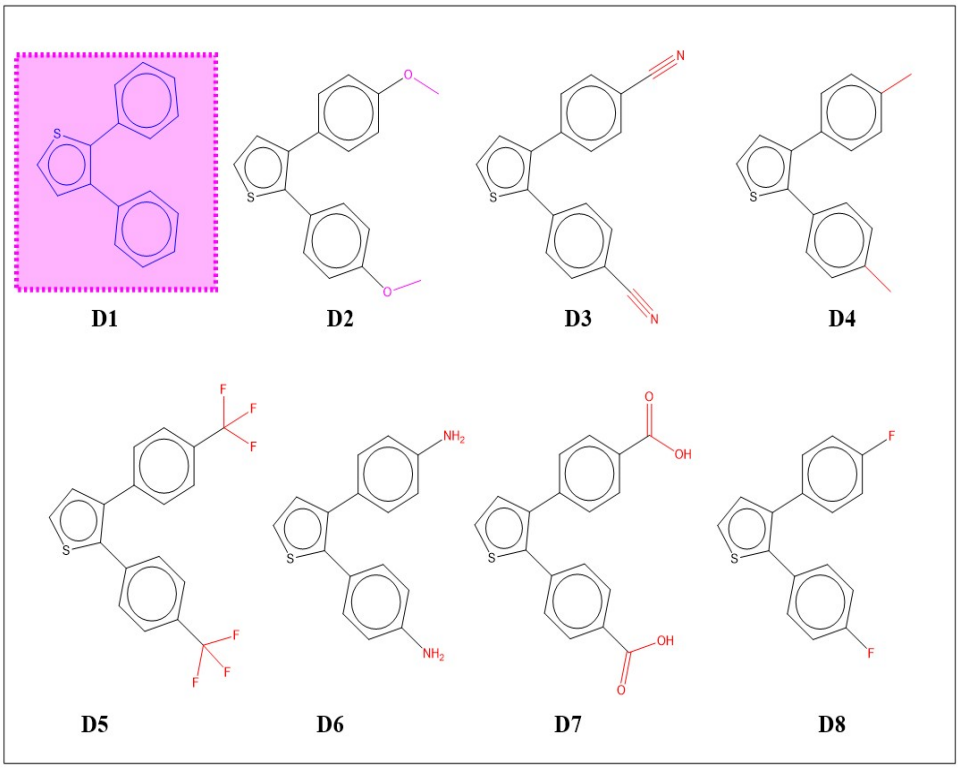

Figure 1: Structure 1: Donor–Acceptor Molecules D1-D8

3.1. Frontier Molecular Orbitals and Energy Gap Analysis

At 298 K, room temperature, the Egap of the molecules studied had values in the range 2.86–3.64 eV, indicating different levels of conjugation and ICT character. Molecules having very strong electron-donating and accepting groups, such as Triphenylamine–BT and Carbazole–TCNE show Egap values of 2.91 eV and 2.86 eV, respectively, while reference-like molecules show a wider gap of 3.52 eV. For example, D1—in a molecule. Temperature was such that it led to a decrease in the HOMO–LUMO gap in more of the molecules. For instance, D3 had its Egap reduced from 2.91 eV at 298 K to 2.79 eV at 348 K; therefore, there would be enhancement in π -conjugation or increase charge transfer due to conformational relaxation. This is typical of thermochromic systems where there can be modulation of electronic transitions by weak thermal perturbations. Interestingly, compounds such as D4 $(Fluorene–NO_2)$ and D8 (TPA–CHO) showed smaller Egap decrease (0.06–0.09 eV) what supports their more rigid aromatic backbones. However, the molecule D6 showed a dramatic gap reduction from 2.86 eV to 2.68 eV, which indicates there is a large reorganization of electron density and orbital alignment, and thus supports its strong thermochromic nature Figure 2.

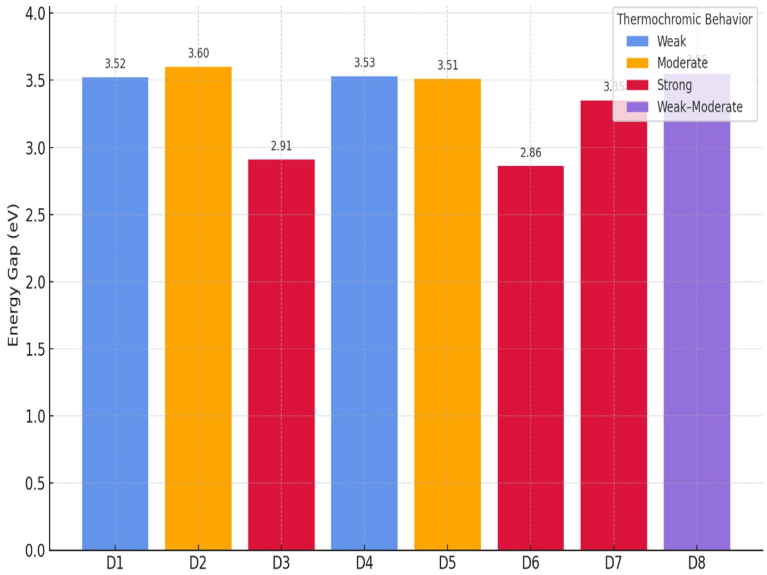

Figure 2: Molecular Orbitals and Energy Gap of D1-D8

3.2. Absorption Maxima and Thermochromic Shifts

The absorption maxima (λmax) of several compounds were found to be very much changed in their values, as seen from the TD-DFT calculations. D1 had a λmax of 354 nm at 298 K; D3 and D6 had absorbance at 398 nm and 412 nm, respectively. The shifts to higher wavelengths show that there is more ICT efficiency because their conjugation is extended and there are stronger donor-acceptor interactions. Upon heating to 348 K, there were observable redshifts; D3's λmax grew to 415 nm, and that of D6 moved to 432 nm, a 17–20 nm shift in both cases. These redshifts point to reduced energy of transition and correspond to an abating HOMO–LUMO gap at higher temperatures. Molecules such as D2 and D5 show moderate shifts (˜10 nm), D4 shows but a small movein (˜4 nm), further driving home the point that it is the combination of structural rigidity and ICT intensity that dictates thermochromic response Figure 3 .

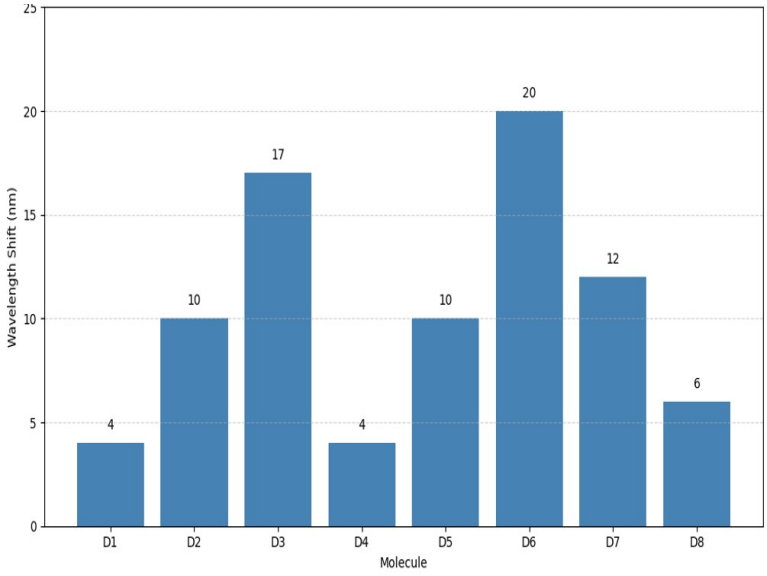

Figure 3: Absorption Maxima and Thermochromic Shifts of D1-D8

A scatter plot of the dipole moment of each molecule against the λ max shift was used to establish a probable relationship in electronic structure and thermochromic response. From Figure 4, it is observable that relatively more polar molecules—D6 (6.18 D) and D3 (5.45 D)—show a spectral shift of 20 nm and 17 nm, respectively. It is most probable that stronger thermochromic behavior results due to enhanced intramolecular charge redistribution in more polar molecules. For relatively less polar molecules, for example, D1 and D4, the observed spectral shifts do not appear to be as great, 7-10 nm, under these conditions, which is suggestive that a different mechanism is at play Figure 4.

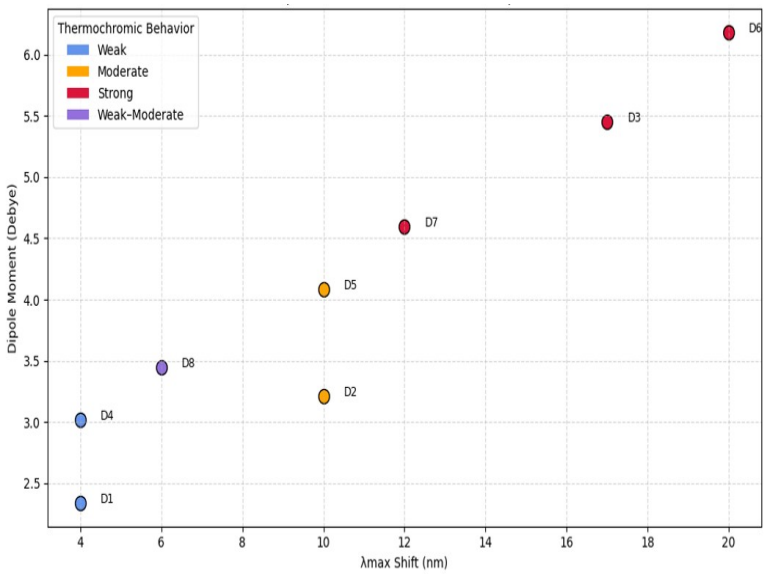

Figure 4: Show moderate shifts of D1-D8

3.3. Orbital Distribution and Charge Delocalization

Frontier orbital views showed that molecules with marked color changes had temperature-dependent orbital distributions. In D3, the HOMO was mostly found over the triphenylamine core at 298 K, while the LUMO was found over the benzothiadiazole unit. At 348 K, however, there was overlap of orbitals which shows increased conjugation and electron delocalization to the whole molecule. Likewise, at high temperature, a more spread out LUMO is seen in D6, indicating more intense electronic coupling between carbazole and the TCNE unit. That change corresponds to the absorption wavelength increase and energy gap decrease that was observed. On the other hand, D1 and D4 show relatively localized orbitals in all cases of excitation; this fact correlates well with their weaker thermochromic behavior Figure 5.

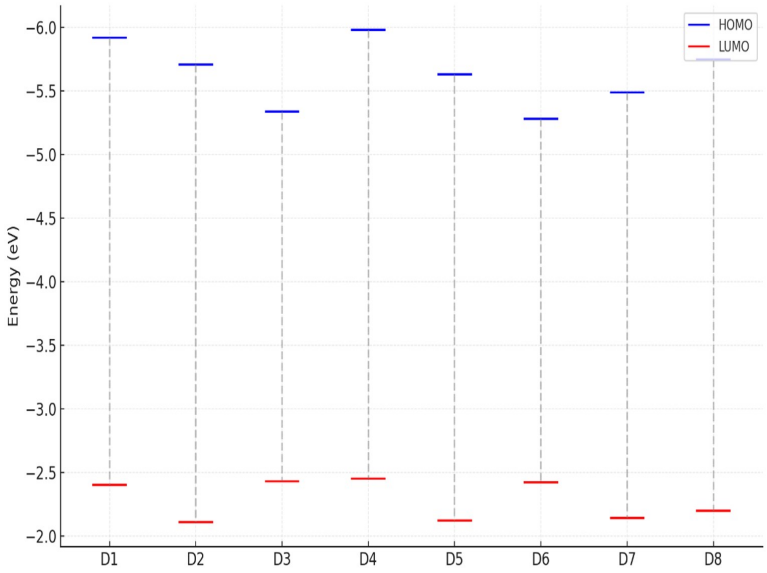

Figure 5: Show moderate shifts of D1-D8

3.4. Thermodynamic Stability and ZPE Corrections

The electronic observations were supported by thermodynamic data. All molecules were confirmed as true minima through frequency analysis. The zero-point energy (ZPE) and values that compounds with more delocalized systems is better thermal stability Gibbs free energy values indicated that compound (D3, D6, D7) exhibited slightly h showed slightly higher thermal stability. For instance, compound D3 had a Gibbs free energy of −950.28 Hartree at 298 K while that for D1 was −932.14 Hartree. an Hartree at 298 K compared to −932.14 Hartree for D1 compound(implies) Such stability implies good structural robustness under moderate heating, a Desirable trait in practical thermochromic materials. Also, entropic contributions rose a little with temperature for all molecules, but none showed any sign of thermal degradation or instability within the range studied, thus confirming the suitability of these molecules for thermal cycling applications.

3.5. Overall Structure–Property Relationships

Among all eight molecules, D3 and D6 show differentiation as the most promising thermochromic candidates with both showing:
a. Narrowing of Egap by $\geq$ 0.12 eV between 298 K and 348 K
b. More than 15 nm redshifts in λmax
c. Temperature-dependent delocalization of FMOs
d. Stable thermodynamic profiles

D7 and D5 also showed good performance though with less spectral changes. Molecules like D1 and D4 indicated minimal electronic reconfiguration upon heating and could be termed stable and non-responding. These differences highlight the role of π-bridge flexibility, donor/acceptor strength, and the molecular planarity random access memory for achieving thermally tunable optoelectronic properties.

3.6. Electronic Properties and Dipole Moment Analysis

To understand better the polarity and potential intramolecular charge separation of the molecules designed, their dipole moments were calculated at the B3LYP/6-31G(d,p) level of theory. Figure 6 shows that the values of dipole moment vary greatly among the compounds, with D6 having the highest polarity 6.18 D, followed by D3 and D7. These results correspond to their strong thermochromic responses observed and support a relationship between enhanced dipole moments and increased color-shifting ability Figure 6.

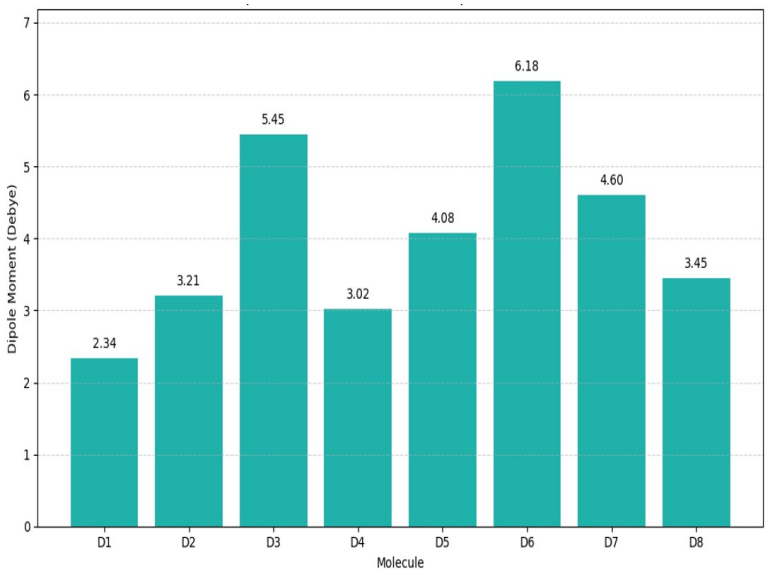

Figure 6: Electronic Properties and Dipole Moment Analysis of D1-D8

4. Conclusion

This theoretical study has dealt with the thermochromic behavior of eight organic donor–acceptor molecules and has carried out exhaustive DFT and TD-DFT simulations. Results revealed that thermal modulation can impose a very large effect on the electronic and optical properties of the D–A systems which concomitantly have extended conjugation and flexible π -bridges. Of the compounds under study, D3 (Triphenylamine–Benzothiadiazole) and D6 (Carbazole–TCNE) are more thermochromic active displaying marked red shifts in absorption maxima, significant diminution of the HOMO–LUMO energy gap with charge delocalization increasing at higher temperatures. These results prove that careful molecular designs that have strong electron-donating and -accepting groups as well as optimized conjugation pathways can show temperature-dependent color changes. Such systems can be useful for several smart applications, including thermal sensors, displays, and optoelectronic devices. The study also shows how quantum chemical tools can be used to predict structure–property relationships before the actual synthesis and thus serve as a guide for the rational design of future thermochromic compounds.

References

[1] S. Hossain, A. Sadoh, and N. M. Ravindra. Principles, properties and preparation of thermochromic materials. *Material Science Engineering International Journal*, 7:146–156, 2023.

[2] S. A. Aksoy, S. Özkayalar, and C. Alkan. Development of hybrid functional thermoregulating and thermochromic microcapsules and polyester textiles. *Energy Storage*, 7, 2025.

[3] A. Hakami et al. Review on thermochromic materials: development, characterization, and applications. *J Coat Technol Res*, 19: 377–402, 2022.

[4] K. Zeng, C. Xue, J. Wu, and W. Wen. Development of advanced solid-state thermochromic materials for responsive smart window applications. *Polymers (Basel)*, 16:2385, 2024.

[5] P. J. J. O'Malley et al. Scalable quantum simulation of molecular energies. *Phys Rev X*, 6:031007, 2016.

[6] A. Molina-Sánchez, M. Palummo, A. Marini, and L. Wirtz. Temperature-dependent excitonic effects in the optical properties of single-layer mos 2. *Phys Rev B*, 93:155435, 2016.

[7] Y. Kim et al. Quantum biology: An update and perspective. *Quantum Reports*, 3:80–126, 2021.

[8] R. Khaledialidusti, B. Anasori, and A. Barnoush. Temperature-dependent mechanical properties of ti n+1 c n o 2 (n = 1, 2) mxene monolayers: a first-principles study. *Physical Chemistry Chemical Physics*, 22:3414–3424, 2020.

[9] M. Bursch, J. Mewes, A. Hansen, and S. Grimme. Best-practice dft protocols for basic molecular computational chemistry**. *Angewandte Chemie International Edition*, 61, 2022.

[10] J. Yago Malo, L. Lepori, L. Gentini, and M. L. Chiofalo. (marilù). atomic quantum technologies for quantum matter and fundamental physics applications. *Technologies (Basel)*, 12:64, 2024.

[11] J. M. Gallmetzer, J. Gamper, S. Kröll, and T. S. Hofer. Comparative study of umcm-9 polymorphs: Structural, dynamic, and hydrogen storage properties via atomistic simulations. *The Journal of Physical Chemistry C*, 129:5645–5655, 2025.

[12] M. Franco-Pérez. The electronic temperature and the effective chemical potential parameters of an atom in a molecule. a fermi–dirac semi-local variational approach. *Physical Chemistry Chemical Physics*, 24:807–816, 2022.

[13] Q. Mao et al. Classical and reactive molecular dynamics: Principles and applications in combustion and energy systems. *Prog Energy Combust Sci*, 97:101084, 2023.

[14] M. Ceriotti et al. Nuclear quantum effects in water and aqueous systems: Experiment, theory, and current challenges. *Chem Rev*, 116: 7529–7550, 2016.

[15] O. Noureddine, N. Issaoui, S. Gatfaoui, O. Al-Dossary, and H. Marouani. Quantum chemical calculations, spectroscopic properties and molecular docking studies of a novel piperazine derivative. *J King Saud Univ Sci*, 33:101283, 2021.

[16] H. Afshar, F. Kamran, and F. Shahi. Advances in smart chromogenic hydrogel composites for next-generation digital applications. *Polym Adv Technol*, 36, 2025.

[17] H. Liang et al. Bio-inspired micropatterned thermochromic hydrogel for concurrent smart solar transmission and rapid visible-light stealth at all-working temperatures. *Light Sci Appl*, 13:202, 2024.

[18] L. Xie et al. Engineering self-adaptive multi-response thermochromic hydrogel for energy-saving smart windows and wearable temperature-sensing. *Small*, 19, 2023.

[19] A. B. M. Supian et al. Thermochromic polymer nanocomposites for the heat detection system: Recent progress on properties, applications, and challenges. *Polymers (Basel)*, 16:1545, 2024.

[20] Y. Zhao et al. Thermochromic smart windows assisted by photothermal nanomaterials. *Nanomaterials*, 12:3865, 2022.

[21] D. Avagliano, M. Skreta, S. Arellano-Rubach, and A. Aspuru-Guzik. Delfi: a computer oracle for recommending density functionals for excited states calculations. *Chem Sci*, 15:4489–4503, 2024.

[22] J. Hafner, C. Wolverton, and G. Ceder. Toward computational materials design: The impact of density functional theory on materials research. *MRS Bull*, 31:659–668, 2006.

[23] A. D. Laurent, C. Adamo, and D. Jacquemin. Dye chemistry with time-dependent density functional theory. *Phys. Chem. Chem. Phys.*, 16:14334–14356, 2014.

[24] J. O. Anhaia-Machado et al. Molecular modeling based on time-dependent density functional theory (td-dft) applied to the uv-vis spectra of natural compounds. *Chemistry (Easton)*, 5:41–53, 2022.

[25] K. P. Zois and D. A. Tzeli. Critical look at density functional theory in chemistry: Untangling its strengths and weaknesses. *Atoms*, 12: 65, 2024.

[26] J. M. Gallmetzer, J. Gamper, S. Kröll, and T. S. Hofer. Supporting information: A comparative study of umcm-9 polymorphs: Structural, dynamic, and hydrogen storage properties via atomistic simulations.

[27] X. Zhang et al. Artificial intelligence for science in quantum, atomistic, and continuum systems. 2023.

[28] M. E. Casida. Time-dependent density-functional theory for molecules and molecular solids. *Journal of Molecular Structure: THEOCHEM*, 914:3–18, 2009. doi:10.1016/j.theochem.2009.08.018. Preprint at.

[29] Y. Luo et al. Phase stability of tio 2 polymorphs from diffusion quantum monte carlo phase stability of tio 2 polymorphs from diffusion quantum monte carlo phase stability of tio 2 polymorphs from diffusion quantum monte carlo 2. http://energy.gov/downloads/doe-public-access-plan.

[30] Y. Kim et al. Quantum biology: An update and perspective. *Quantum Reports*, 3:80–126, 2021.

[31] S. G. Balasubramani et al. Turbomole: Modular program suite for ab initio quantum-chemical and condensed-matter simulations. *J Chem Phys*, 152, 2020.

[32] J. Nyman and G. M. Day. Modelling temperature-dependent properties of polymorphic organic molecular crystals. *Physical Chemistry Chemical Physics*, 18:31132–31143, 2016.